Research on Engineering Structures & Materials
www.jresm.org
Research Group

Research Article

Influence of SiO_2 and nano graphene particles on the microstructure and mechanical behavior of A356 alloy metal composites

Samuel Dayanand[1,a], S Manjunath Yadav[1,b], Madeva Nagaral[2,c], Satish Babu Boppana[3,d], Manjunatha T H[4,e], V Auradi[5,f]

[1]*Dept. of Mechanical Engineering, Government Engineering College, Karnataka, India*
[2]*Aircraft Research and Design Centre, Hindustan Aeronautics Limited, Karnataka, India*
[3]*Dept. of Mechanical Eng., School of Eng. College, Presidency University, Karnataka, India*
[4]*Dept. of Mechanical Eng., Ballari Institute of Technology and Management, Karnataka, India*
[5]*Department of Mechanical Engineering, Siddaganga Institute of Technology, Karnataka, India*

Article Info

Article history:

Received 06 Nov 2023
Accepted 18 Apr 2024

Keywords:

A356 alloy;
Metal matrix composite;
Stir casting;
Tensile properties;
Silicon oxide;
Graphene

Abstract

The current research focuses on investigating the microstructural and mechanical properties of aluminum (Al) metal matrix composites (MMCs) reinforced with both silicon dioxide (SiO_2) and nano-graphene particles. The composite material was produced using a novel two stage stir cast metallurgy approach. In this study, a constant reinforcement of 1 wt. % nanographene was maintained, while the SiO2 content was independently varied at levels of 2.5, 5, and 7.5 wt. %. Employing scanning electron microscopy (SEM) tool, microstructural analyses were conducted, revealing a uniform dispersion of ceramic silicon dioxide (SiO2) and graphene particles within the as-cast A356 MMCs. Mechanical testing, following the ASTM standards, was carried out on the composites, specifically assessing tensile strength, yield strength, and percentage elongation to evaluate the properties of the Al-based MMCs. The findings of this study indicate a significant enhancement in both tensile and yield strength values for the fabricated composites by 60.64% and 82.78% respectively. However, it is important to note that the percentage elongation decreases as the reinforcement content in the composite increases.

1. Introduction

In recent times, there has been remarkable growth in the development of materials used for various engineering applications. Traditional engineering materials, which are often unmodified monolithic substances, may not be suitable for certain specialized applications. Consequently, composite materials have emerged as innovative solutions to meet the requirements of such applications [1]. Researchers are actively engaged in combining advanced materials and novel processing techniques to create a new category of metal matrix composites (MMCs). These customized composite materials find specific applications in sectors like aviation, defense, and the automotive industry, owing to their unique and significantly enhanced properties compared to solid materials. The distinctive properties of Al-based MMCs, such as their low weight and high strength, make them highly relevant in the realm of engineering materials. One of the most significant advantages of composite materials is the ability to tailor their properties by choosing suitable reinforcements [2]. Researchers have used a variety of matrices and reinforcement

*Corresponding author: madev.nagaral@gmail.com
[a] orcid.org/0000-0001-5279-3522; [b] orcid.org/0000-0003-2358-4005; [c] orcid.org/0000-0002-8248-7603; [d] orcid.org/0000-0002-1792-2621; [e] orcid.org/0000-0002-2794-797X; [f] orcid.org/0000-0001-6549-6340
DOI: http://dx.doi.org/10.17515/resm2024.73me1106rs

systems when dealing with MMCs. Powder metallurgy and liquid metallurgical techniques are employed to refine these composites [3, 4]. Integrating hard or soft ceramic or nonmetal reinforcements into aluminum alloy is a huge challenge, according to the research. By employing an optimized fabrication technique, wetting properties and homogenous reinforcement particle dispersion inside the matrix can be achieved in aluminum-based composites [5, 6]. Vasant Kumar et al. [7] investigated the impact of SiC particles inclusion on the mechanical behavior of Al2014 alloy composites. These composites were fabricated by using 5 and 10 wt. % of SiC particles with liquid metallurgy route. Al2014 alloy with 10 wt. % of SiC composites exhibited the superior properties.

Aluminum is the most commonly used matrix material for MMCs, as it offers several desirable attributes, including low density, excellent thermal and electrical conductivity, precipitation hardening capability, corrosion resistance, and high damping capacity. Moreover, it offers an extensive range of mechanical properties, depending on its chemical composition. Al-based MMCs are usually strengthened with ceramic particulates, such as Al_2O_3, SiC, B, AlB_2, TiB_2, BN, SiO_2, AlN, and others. Various fabrication methods, predominantly based on casting or powder metallurgy, are available for creating nano-size (or micro-size) particle/metal composites [8, 9]. However, achieving uniform dispersion of particles in liquid metal can be challenging. Furthermore, micro-level porosity, a common casting defect, can pose difficulties in creating micro-level geometries [10].

Silicon oxide (SiO_2) is one of the most cost-effective and readily available reinforcements, capable of retaining high strength at elevated temperatures and offering excellent mechanical and wear properties [11]. Silica has diverse applications in various fields, containing drug delivery systems, catalysis, biomedicine, imaging, chromatography, sensors, and as a filler in composite materials [12]. It is also used for porous silica ceramics, which serve as high-temperature dielectrics and thermal shields, with applications in aerospace and engineering [13]. Silica enhances the strength and hardness of ceramic materials [14]. Additionally, silica aerogel, due to its porous, ultra-lightweight, and nanostructured properties, is utilized in composite insulators and for water resistance, UV protection, fire resistance, and acoustic barriers [15]. Silica gel, known for its great specific surface area and gas adsorption capacity, is employed as an adsorbent for heavy metal removal from wastewater and the adsorption of volatile organic compounds. In various applications, silica nanoparticles are employed as super-hydrophobic materials by modifying their hydrophilic properties to hydrophobic ones [16].

Graphene, on the other hand, stands out due to its exceptional conductivity, high Young's modulus, high specific surface area, and high electron mobility. Carbon atoms are packed tightly into a honeycomb lattice arrangement in a single layer [17]. Since graphene's discovery, there has been constant investigation into new methods of synthesis to meet the needs of a wide range of industries, such as the automotive, green energy, electronics, biomedical, and catalyst fields [18]. To improve the thermal conductivity of aluminum matrices, graphene shows promise as a reinforcement due to its high thermal conductivity. Graphene tends to settle to the bottom and may not scatter uniformly [19], therefore there have been challenges in exploring graphene-reinforced composites utilizing liquid stirring methods. Researchers have been working to improve the mechanical and wear properties of MMCs by creating hybrid-reinforced variants. To fulfill the needs of future sophisticated applications, the next generation of such materials includes these hybrid aluminum AMCs [20].

Hybrid composites have been developed through additional testing, with the goal of improving mechanical qualities such as dimensional stability and heat and corrosion resistance by merging two or more reinforcement components [21]. Many hybrid composites have had their mechanical properties studied, and the results demonstrate that

the tensile strength, stiffness, and porosity all increase with the percentage of reinforcement in the matrix. Impact energy and composite density are both greatly reduced, however, with increasing reinforcing content. Several investigators were studied various properties of MMCs.

In their investigation, Knowels et al. [22] examined the mechanical properties of 6061 alloy that had been made using the powder metallurgy technique and had SiC nano particles added to it. The mechanical qualities are enhanced by the powder metallurgy process, which distributes the particles without clumping. The Young's modulus was greatly enhanced after 8 hours of heat treatment at 125˚C, which led to a strong connection between the particles and the matrix. A combination of high strength, hardness, and ductility was achieved by adding tiny SiC particles (less than 500 nm in size). An aluminum composite including Al_2O_3 particles was created by Dinesh Kumar Koli et al. [23] through the use of ultrasonic assisted casting. Maintaining the microstructure while controlling the grain size is no easy feat. Various processes are examined in this research. Better bonding, easier microstructure control, and reduced cost are all benefits of ultrasonic aided casting. Nano alumina particles, when added up to 4% by volume, increase the strength until it plateaus.

The copper composites enhanced with SiC were made by Mohsen et al. [24] utilizing the friction stir method. Through optical and scanning electron microscopy, the existence of SiC particles was captured. The incorporation of silicon carbide particles into the copper matrix improved its wear resistance. A study comparing the wear behavior of brake shoe linings made of grey cast iron and aluminum alloy 356 strengthened with a 25% silicon carbide metal matrix composite was carried out by Natarajan et al. [25]. Grey cast iron brake shoe linings from passenger cars were cut to a diameter of 10 mm and tested beside MMC coated with AA356-25 wt. % SiC particles. Researchers used the pin-on-disc technique to study tribological behavior and discovered that MMC wore out less quickly than grey cast iron. It was also discovered that, under same circumstances, the frictional force of MMC sliding was 20% greater than that of cast iron, which would improve braking.

The composition material studied by Raghu et al. [26] is made up of A356 alloy with silicon carbide particles in weight percentages of 3, 5, 7, and 10. The powder metallurgy procedure was used to process the material. Hardness, tensile strength, and compression strength all rose with increasing weight percentages of SiC particles, with maximum values shown at 10 weight percent of SiC, according to scanning electron microscopy data. The SiC was found to disperse very uniformly throughout the A356 matrix. At 10 weight percent SiC, the wear rate was likewise determined to be minimal. Using the salt metal reaction in-situ approach, Mingliang Wang et al. [27] created a composite of A356 matrix alloy and titanium di boride (TiB_2) particles in both their as-cast and T6 heat-treated forms. The characteristics of A356/TiB_2 composites were enhanced. As TiB_2 particles were added to the composite, a smaller average grain size was noted.

Given the distinct advantages of both graphene and silica, their integration has been projected to achieve superior properties. The synthesis of graphene-silica hybrid composites combines the strengths of both materials while mitigating issues related to graphene agglomeration [28]. Agglomeration can significantly reduce the surface area of graphene, diminishing its performance.

Based on the literature review wettability and agglomeration are the major problems in the processing of metal composites. In the present research to overcome these problems novel two step stir casting process has been adopted to prepare the hybrid composites. In this, instead of adding reinforcement particles in single step, entire reinforcement quantity is divided and added into the molten metal in two stages. Two-step process helps in developing good quality castings and enhances the properties. The combination of

graphene and silica effectively addresses this challenge and results in advanced functional materials. Such composites are extensively used in applications such as electrodes, catalysts, hydrogen storage, batteries, displays, adsorbents, and sensors. Notably, researchers have explored the mechanical possessions of composites using A356 with SiO_2 and graphene as reinforcements, which is a relatively less explored area [29].

2. Experimental Details

2.1 Matrix and Reinforcement Materials

In this particular study, A356 was designated as the matrix material due to its varied range of applications in the automotive and aviation industries. The A356 matrix was reinforced with a combination of silicon oxide (SiO_2) and graphene. Graphene was kept constant at 1 wt. %, while the SiO_2 content was varied at levels of 2.5, 5, and 7.5 wt. % of the matrix material, leading to the development of hybrid metal composites. The chemical composition of A356 is detailed in Table 1 and the A356 material was sourced from Fenfee Metallurgical Pvt. Ltd, located in Bangalore, Karnataka, India. The SiO_2 particles employed in this research had particle size of 35µm. Through the addition of varying percentages of the (SiO_2 + Graphene) mixture in different combinations, we successfully produced Al-SiO_2-Gr hybrid composites. Fig. 1 is indicating the process adopted to prepare A356 alloy composites.

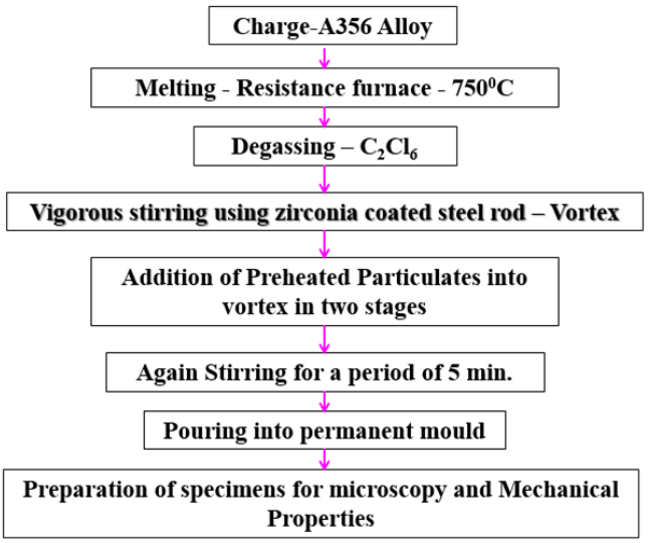

Fig. 1. Process of preparing A356 alloy hybrid composites

Table 1. Chemical composition of A356 alloy [30]

Constituent	Si	Mg	Fe	Cu	Zn	Mn	Ti	Al
Wt. %	7.5	0.45	0.2	0.2	0.1	0.1	0.05	Balance

2.2 Composite Fabrication

The specimen preparation involved employing the standard stir-casting method. In the production of each sample, 2000 grams of aluminum (A356) were melted using a graphite crucible in an electric furnace with an argon environment, maintaining a temperature of

750°C. To achieve a homogeneous melt, the furnace temperature was consequently amplified to 850°C and maintained for 20 minutes. Furthermore, to enhance the wettability of the matrix alloy with the reinforcements, 0.5 wt.% of magnesium was introduced into the molten metal. In order to oxidize the surface of the SiO_2 particles, they underwent a baking process for 3-4 hours at a temperature of 200°C in a baking oven. This preheated powder was then fed into the molten metal at a consistent feed rate using Gr powder and mixed uniformly with the molten metal by a graphite stirrer rotating at 400 rpm for approximately 5 minutes.

(a) (b)

Fig. 2. Showing the (a) Molten metal in electric furnace (b) Cast iron die used to prepare samples

This ensured an even distribution of the particles throughout the metal. The constant reinforcement of graphene (1 wt.%) was introduced into the molten metal through an external sprue. The graphene and SiO_2, with particle sizes of 10 nm, were added to the molten matrix at varying wt.% levels (2.5, 5, and 7.5 wt.%). As the temperature of the molten metal increased to 850°C, the stirring speed was maintained at 500 rpm with a stirring time of 15 minutes to ensure the homogeneous distribution of the reinforcement in the molten matrix. Subsequently, the temperature was raised to 950°C, while the stirring speed and stirring time were increased to 600 rpm and 20 minutes, respectively, to achieve a uniform circulation of the strengthening in the matrix material. In order to avoid heterogeneity and facilitate proper cooling, the steel die was preheated to 350°C.

Fig. 3 A356 alloy hybrid composites

The synthesized aluminum hybrid composite slurry was then poured into the steel die and allowed to cool at atmospheric temperature. A 120 mm length and 15 mm diameter cast iron mold was used for pouring the liquid mixture. The resulting hybridized composite was permitted to harden at ambient temperature before being removed from the mold for subsequent mechanical testing. Samples containing Gr and SiO_2 composites were prepared

using the same procedure for the sake of comparison. Table 2 is representing various composites prepared using A356 alloy with nano graphene and SiO_2 particles. Material A is as-cast A356 alloy, B is A356 alloy with 1 wt. % of graphene and 2.5 wt. % of SiO_2 particles, C is A356 alloy with 1 wt. % of graphene and 5 wt. % of SiO_2 particles and finally, D is A356 alloy with 1 wt. % of graphene and 7.5 wt. % of SiO_2 particles reinforced composites. Fig. 2 (a) is showing the molten metal in the furnace, further Fig. 2(b) is representing cast iron die used to prepare composites. Fig. 3 indicates the prepared casting for the study.

Table 2. List of composites prepared for the study

Sl .No.	Material Code	Composition
1	A	As-Cast A356 Alloy
2	B	A356 + 1 wt. % Gr + 2.5 wt. % SiO2
3	C	A356 + 1 wt. % Gr + 5 wt. % SiO2
4	D	A356 + 1 wt. % Gr + 7.5 wt. % SiO2

2.3 Testing

A comprehensive microscopic analysis of the newly synthesized hybrid composites is crucial to gain a deeper understanding of their microstructural characteristics. To examine the microstructure of the Al-SiO_2-Gr hybrid composites, specimens were prepared following the ASTM standard for metallographic procedures. The microstructures were inspected using a scanning electron microscope (SEM). The samples were etched using Keller's Reagent (HF /HCl/HNO_3/H_2O), and emery paper with varying grades (400, 600, and 1000) was employed in the preparation process. SEM analysis was performed to measure the microstructure and the uniform dispersion of SiO_2 and graphene particles in the hybrid composites. For microstructural examination, cylindrical samples were produced, with dimensions of 10 mm in diameter and 5 mm in height for SEM images. The microstructure samples, as shown in Figure 4, were an integral part of the research, and the VEGAS TESCAN scanning electron microscope was used for microstructural analysis. The tensile properties of the composites were examined in accordance with the ASTM-E8 standard [31]. Furthermore, the tensile and compressive properties of the aluminum hybrid composite were evaluated following the ASTM E9 standard [32]. During the testing, ambient conditions were maintained, with temperatures ranging from 25°C to 30°C and relative humidity levels between 40% and 60%. A computerized universal testing machine (Instron 5982) equipped with a strain gauge extensometer was employed, and the tests were conducted at a constant cross-head speed of 1 mm/min at room temperature. Impact tests were showed using Charpy specimens measuring 56 × 10 × 10 mm, with a 3 mm notch depth, a tip radius of 0.30 mm, and angles of 45°, on impact testing machines. To obtain an average result, all specimens underwent three evaluations for both hardness and impact strength. Brinell hardness tests were carried out using a 5 mm ball diameter and a load-carrying capacity of 250 kg. The hardness test involved specimens measuring 15 mm in diameter and 10 mm in thickness.

3. Results and Discussion

In this current investigation, we have undertaken the synthesis of aluminum composites with SiO_2 and Graphene particles. The composition includes a consistent 1 wt.% of graphene and varying SiO_2 content at levels of 2.5, 5, and 7.5 wt.%, and the production method employed is the stir casting technique. Comprehensive experimental studies have been carried out, encompassing microstructural analysis, tensile strength assessment,

compressive strength evaluation, impact and hardness testing. The results and analysis of these synthesized hybrid composites are elaborated in the subsequent section.

3.1 Microstructural Analysis

To analyze the morphologies of SiO_2 and graphene particles, we employed SEM micrographs. SiO_2 particles exhibited spherical shapes, as apparent in the micrographs. Fig. 4 (a) to (d) illustrate the SEM micrographs of A356 alloy, A356-2.5 wt.% SiO2-1 wt.% graphene, A356-5 wt.% SiO2-1 wt.% graphene, and Al-7.5 wt.% SiO_2-1 wt.% graphene, respectively. The images in Fig. 4(b) and (d) depict SiO_2/graphene particles as round and spherical particles. The spherical morphology confirms the presence of SiO_2 particles and nano-graphene within the matrix. The grain boundaries in Fig. 4 (a) to (c) appear dendritic, suggesting an even dissemination of the reinforcing particles throughout the composite and alloy. Within all the microstructures, fine precipitates are observed in the alloying components, scattered along the grain boundaries in the A356 composite framework. Notably, clusters of SiO_2 and graphene particles are dispersed throughout the matrix. These micrographs reveal the fine distribution of SiO_2 and graphene particles, which is a result of careful selection of appropriate mixing/stirring time and method during casting.

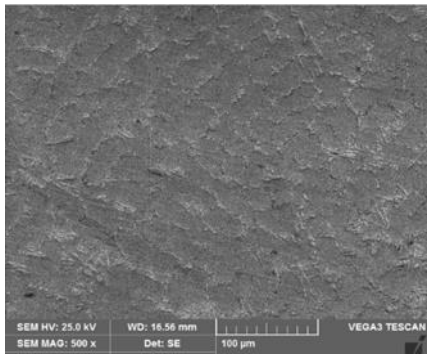

(a)

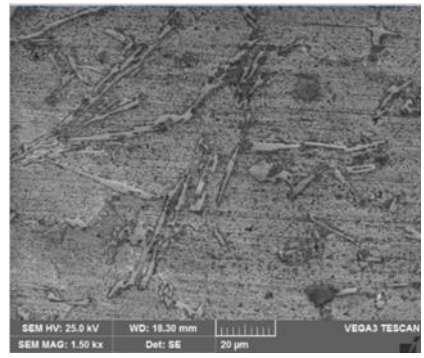

(b)

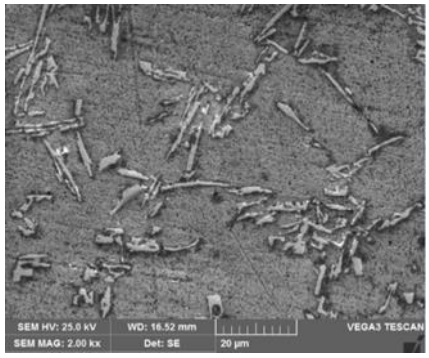

(c)

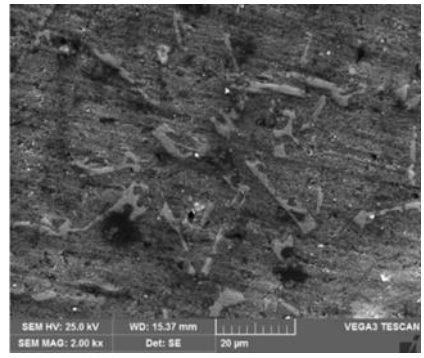

(d)

Fig. 4. SEM Micrographs of (a) As-cast A356 alloy (b) A356-1 wt.% of Gr and 2.5 wt.% of SiO_2 Composites (c) A356-1 wt.% of Gr and 5 wt.% of SiO_2 Composites(d) A356-1 wt.% of Gr and 7.5 wt.% of SiO_2 Composites

Graphene particles are typically found interspersed between dendrites. Most SiO2 particles exhibit spherical, angular, or sub-angular shapes, and occasionally, a plate-like

structure similar to graphene is observed. The micrograph clearly shows that SiO2 and graphene platelets are evenly dispersed in the matrix, with no signs of clustering. The excellent interfacial bonding is attributed to pre-warming the SiO_2 and graphene particles before presenting them into the molten material. In Fig. 4(a), we observe the micrograph of the alloy used, revealing a dendritic form. The base matrix contains a white light-Al phase with precipitates both inside and outside the grains. The Fe-Mn-Si-Al phase of the alloy predominantly appears on the alloy's surface. In Fig. 4(b), the micrograph highlights the faceted features of SiO2 crystals, known for their monoclinic crystal structure at room temperature, transitioning to a tetragonal and cubic structure at higher temperatures. Fig. 4(c) pertains to the graphene reinforcement, showing stacked layers with a crumpled appearance.

In the SEM micrographs (Fig. 4), it is noticeable that intergranular porosity is present, but there is a well-formed microstructure due to strong bonding between the aluminum matrix and SiO_2/graphene particles. The grain boundaries are clearly discernible in the sample, and the inter-particle bonding is robust. In Fig. 4(b), the micrograph of the sample reveals a compact microstructure with minimal porosity. Therefore, the improved bonding between the particles and reduced porosity may contribute to an increase in the load-bearing capacity of the composite specimens. The distribution of grey SiO_2 particles can possibly be attributed to the high thermal conductivity of the alloy steel die, which enhances the solidification process. However, increasing the graphene content could potentially lead to more agglomeration and an increase in porosity. Additionally, a significant mismatch exists between aluminum and graphene, which could result in debonding at the interface. The graphene particles, due to their exceptionally high conductivity, may appear significantly brighter compared to the surrounding microstructure of the composite sample. The dendritic microstructure observed reflects the morphology resulting from the interaction between aluminum and graphene particles during the casting process. This interaction might be influenced by the formation of carbide phases, as reported in prior studies [33].

3.2. EDS Analysis

Energy dispersive X-ray spectroscopy (EDS) is a valuable technology for determining the composition and relative proportions of elements. While chemical analysis can recognize the existence of elements in a sample, quantifying their proportions can be challenging, making EDS an essential tool. In this study, EDS was employed to perform elemental analysis on A356 composite materials reinforced with 1 wt.% graphene and 2.5, 5, and 7.5 wt.% SiO_2. The EDS examination was conducted to assess the distribution of reinforcements within the matrix. The EDS peaks indicate the presence of silicon and oxygen, which correspond to the SiO_2 reinforcement (Fig. 5 (a)). This suggests a strong interaction between the reinforcements and the matrix. The carbon peaks are associated with the graphene content. A quantitative analysis of the samples (Fig. 5 (b)) further confirms the presence of these elements. The results of this analysis reveal the essential composition of the A356 composite, including elements such as Al, Mg, Si, Zr, and O, along with the carbon peak. The calculated elemental composition (Fig. 5 (b)) clearly indicates a uniform dispersion of SiO_2 and graphene within the aluminum matrix material.

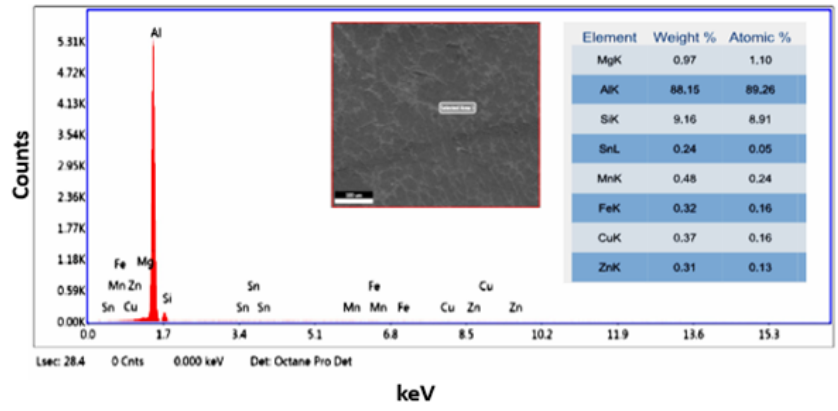
Counts
keV
Al
Fe Mg
Mn Zn
Sn Cu
Si
Sn
Sn Sn
Fe
Mn Mn Fe
Cu
Cu Zn
Zn
Element Weight % Atomic %
MgK 0.97 1.10
AlK 88.15 89.26
SiK 9.16 8.91
SnL 0.24 0.05
MnK 0.48 0.24
FeK 0.32 0.16
CuK 0.37 0.16
ZnK 0.31 0.13
Lsec: 28.4 0 Cnts 0.000 keV Det: Octane Pro Det

(a)

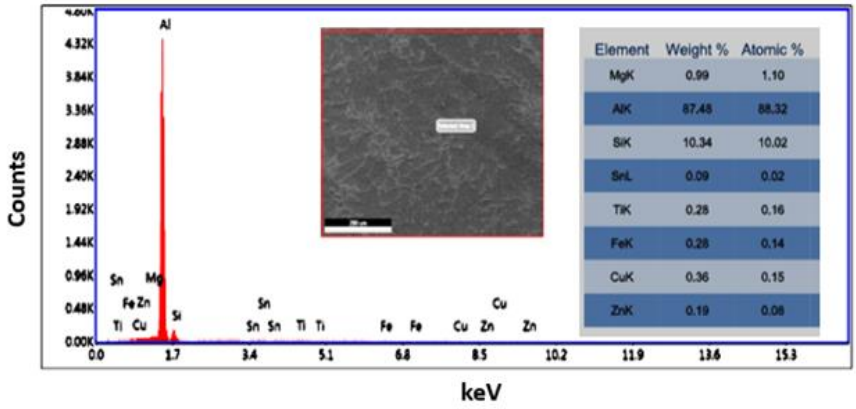
Counts
keV
Al
Sn Mg
Fe Zn
Ti Cu
Si
Sn
Sn Sn Ti Ti
Fe Fe
Cu
Cu Zn
Zn
Element Weight % Atomic %
MgK 0.99 1.10
AlK 87.48 88.32
SiK 10.34 10.02
SnL 0.09 0.02
TiK 0.28 0.16
FeK 0.28 0.14
CuK 0.36 0.15
ZnK 0.19 0.08

(b)

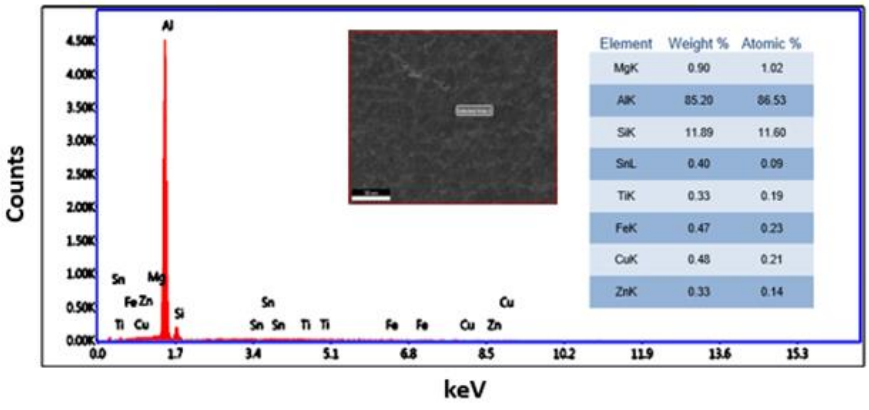
Counts
keV
Al
Sn Mg
Fe Zn
Ti Cu
Si
Sn
Sn Sn Ti Ti
Fe Fe
Cu
Cu Zn
Element Weight % Atomic %
MgK 0.90 1.02
AlK 85.20 86.53
SiK 11.89 11.60
SnL 0.40 0.09
TiK 0.33 0.19
FeK 0.47 0.23
CuK 0.48 0.21
ZnK 0.33 0.14

(c)

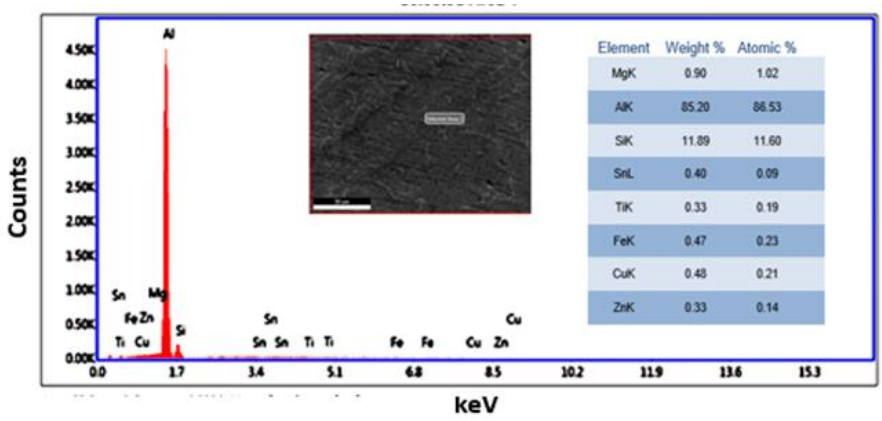

(d)

Fig. 5. EDS analysis of (a) As-cast A356 alloy (b) A356-1 wt.% of Gr and 2.5 wt.% of SiO2 Composites (c) A356-1 wt.% of Gr and 5 wt.% of SiO2 Composites(d) A356-1 wt.% of Gr and 7.5 wt.% of SiO2 Composites

3.3 Tensile Properties

The composites were subjected to room temperature tensile testing in line with the ASTM E-8 standard. Errors were kept to a minimum by carefully preparing three sets of standard specimens and averaging the results. Figure 6 displays the results, which show that the synthesized hybrid composites have expressively higher tensile and yield strength than the monolithic A356 alloy. The ultimate strength of as cast alloy (A) is 116.4 MPa, the increased proportion of SiO_2 reinforcement, the existence of nano graphene particulates, the uniform dispersion of reinforcements within the microstructure, the strong interfacial bonding between the matrix and the reinforcements, the grain size, and the strain gradient strengthening effect are all likely contributors to the observed improvement with 186.9 MPa in case of composite D (1 wt. % of Gr+7.5 wt.% of SiO_2).

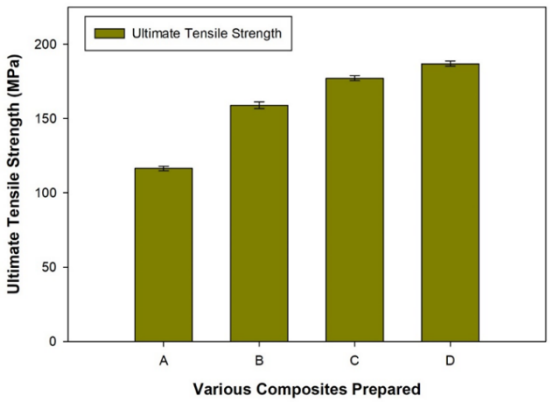

Fig. 6. Ultimate tensile strength of A356 alloy with nano graphene and SiO_2 particles reinforced composites

Recrystallization of the A356 aluminum alloy is facilitated by the addition of strong ceramic reinforcements, which act as nucleation sites. One reason for this is the presence

of reinforced particles, which serve as nucleation sites and prevent the movement of grain boundaries. This results in smaller matrix grain sizes compared to unreinforced A356 alloy. Dislocation motion is effectively slowed by the grain boundaries within the artificially produced aluminum hybrid composites. Grain size is decreased, dislocation accumulation is avoided, and the hybrid composites are strengthened as a whole thanks to suspended dislocations that move continually through the matrix. The tensile behavior of an alloy is also profoundly affected by the incorporation of graphene and SiO_2. Notably, as the weight percentage of SiO_2 particles in the graphene composites increases, the percentage of elongation reduces in aluminum hybrid composites. This is because SiO_2 particles are inherently brittle, which reduces their ductility. As more SiO_2 particles are combined into the graphene composites, the hybrid composites' ductility decreases because the aluminum matrix is less fluid.

The observed increase in the ultimate tensile strength (UTS) can be attributed to the presence of robust SiO_2 and nano graphene particles within the aluminum matrix. These rigid SiO_2 and nano graphene particles contribute to the overall strength of the aluminum matrix through their reinforcing mechanisms. Specifically, they facilitate the transfer of loads from the reinforcement particles to the matrix, resulting in heightened resistance to tensile stress. One key factor contributing to the enhanced strength of the aluminum matrix composites (AMCs) is the notable difference in thermal expansion coefficients amongst the matrix and the reinforcement particles. This disparity in thermal expansion characteristics leads to the development of a higher dislocation density within the matrix. Consequently, the load-bearing capacity of the hard reinforcement particles is increased, elevating the overall strength of the AMCs. As the content of reinforcement particles with a low coefficient of thermal expansion (CTE) rises within a matrix with a higher CTE, microstructural changes occur within the matrix, further contributing to the strength of the material. Additionally, the remarkable strength of the Al-nano Gr-SiO_2 hybrid composite can be attributed to the presence of SiO_2 particles uniformly distributed within the composite matrix, leading to dislocation pile-up in their vicinity. Consequently, the strength of the composite is enhanced due to an increased level of dislocation interactions and dislocation density near the interfaces of the matrix and reinforcement.

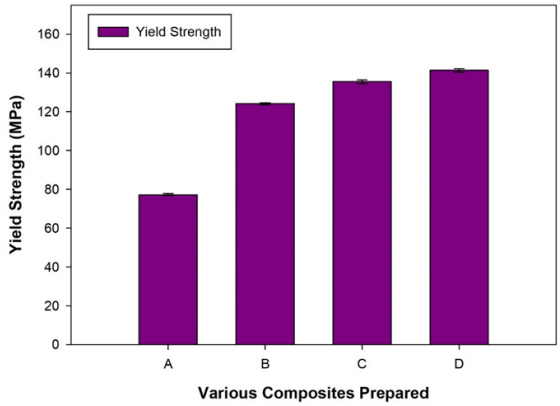

Fig. 7. Yield strength of A356 alloy with nano graphene and SiO_2 particles reinforced composites

The observed behavior can be best explained by deformation strengthening of the hybrid composites, which, despite being inherently brittle, exhibit higher strength and elongation when combined with SiO_2 particles. This effect is consistent with the Hall-Petch relationship, which is influenced by the size of the Gr particles [34]. The influence of

particle size on tensile strength can be elucidated through dislocation theory. The formation of plastic deformation necessitates the overcoming of the ultimate stress, often associated with a mass of moving dislocations. However, grain boundaries hinder dislocation glide, leading to dislocation pile-up. Once the content of dislocation pile-up reaches a certain threshold, it becomes the driving force for dislocation glide. With larger SiO_2 particle sizes, there is a higher content of dislocation pile-up, resulting in a greater driving force for dislocation glide. Smaller Gr particle sizes increase the number of particle boundaries, significantly hindering dislocation motion, and thus influencing the UTS for plastic deformation. The Fig. 7 illustrates the variations in yield strength as a function of the wt. fraction of Gr+SiO_2 reinforced composites. The yield strength, characterized by the stress associated with a plastic strain of 0.2%, exhibits an increase with higher weight fractions of SiO_2 reinforced composites. Remarkably, the A356 with 1 wt. % of Gr and 7.5 wt. % of SiO_2 composite demonstrates notably high yield of 141.4 MPa as compared to the base yield strength of 77.3 MPa.

As can be seen in Fig. 8, the elongation of the composites is significantly altered by the incorporation of SiO_2 and Gr particles into the aluminum alloy. Composites have a lesser percentage of elongation than the metal they are based on reinforcement particles. As the percentage of SiO_2 in the aluminum alloy is raised to 7.5 wt %, however, the composites' elongation drastically decreases, falling to around 32.3%. This decrease in elongation can be traced back to the incorporation of SiO_2 and Gr particles into the aluminum matrix, which reduces the composites' ductility in general [35].

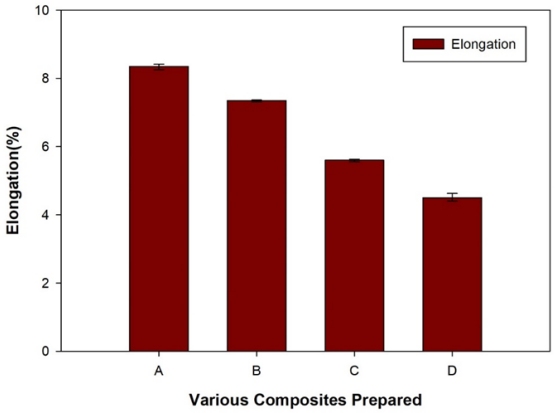

Fig. 8. Yield strength of A356 alloy with nano graphene and SiO2 particles reinforced composites

Figure 8 shows how the ductility of A356 alloy and its composites is affected by the addition of micron-sized SiO_2 and Gr particles. The ability of a material to lengthen under an axial load is referred to as its ductility. The elongation value in tensile testing is found by dividing the gauge length after fracture by the initial gauge length. Material ductility is often given as a percentage, with a larger value indicating greater ductility. Figure 8 shows the % elongation of the as-cast A356 with different wt. % of micron-sized SiO_2 and Gr particles. The percentage elongation of A356 alloy is decreased by the incorporation of SiO2 and Gr particles. As the reinforcing fraction in A356 alloy rises, this decrease becomes more pronounced. The presence of stiff, brittle particles within the A356 alloy matrix is principally responsible for the reduced ductility [36].

3.4 Compressive Strength

Following the ASTM E9 standard, the manufactured aluminum hybrid composites were compressed at room temperature. Compressive strength in A356-SiO_2-Gr composites was expressively improved by the addition of SiO_2 and Gr to the matrix. It is crucial to understand that a metal composites compressive strength almost always exceeds its ultimate tensile strength. This causes these MMCs to be significantly more brittle than monolithic materials, with percentage elongation values typically falling below 5%. The compressive strength data supports earlier findings and demonstrates a notable improvement over the cast hybrid composites with constant reinforcement. The outstanding compression strength of ceramic particles, such as SiO_2, is more characteristic than their tensile strength. In example, the compression strength of SiO_2 particles is much higher than that of the Al matrix. Because of this inherent reinforcing activity, the material is able to successfully resist compressive loads that are given to it. The composite's resistance to compression increases with the fraction of these particles within the foundation material. This is because the bigger volume occupied by the particles reduces the force that can be applied to the matrix, preventing it from deforming. Because the SiO_2 and Gr particles are evenly disseminated throughout the alloy matrix, the hybrid composites' increased compressive strength can be attributable to the twofold strengthening effect. Grain size in the microstructure is diminished because of the presence of these reinforced particles within the aluminum matrix. This effect also aids in the diminution of particle size, which becomes gradually important when particle accumulation heightens [37].

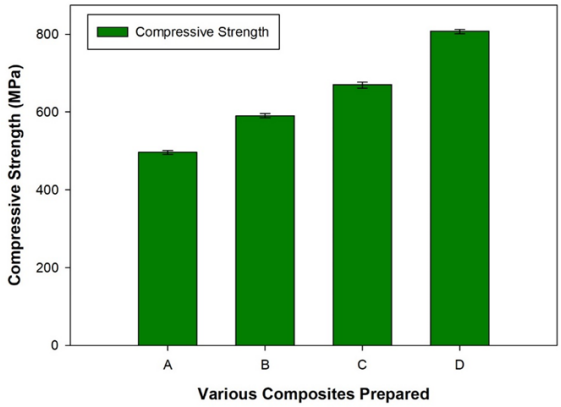

Fig. 9. Compressive strength of A356 alloy with nano graphene and SiO_2 particles reinforced composites

A greater interfacial area is formed between the SiO_2 + Gr reinforcement particles and the Al matrix as the fraction of SiO_2 + Gr reinforcement particles within the matrix increases. As the interface grows, dislocations build up along its edges, mimicking the behavior of grain boundaries. The overall strengthening impact is determined in large part by the inclusion of Gr and SiO_2, which work hand in hand with the distribution strengthening effect. This helps increase the dislocation density in the aluminum matrix and expand the grain size. As can be seen in Fig. 9, the combined effects of these parameters lead to the impressively high compressive strength of the synthesized hybrid composites. According to the reported findings, the compression strength of the A356 alloy matrix is greatly improved by the presence of hard particle phases, and this improvement is magnified as the percentage of SiO_2 + Gr particles increases. Compressive strength is a common measure of the durability of carbide or oxide particles due to the intrinsic hardness of ceramics.

Strength enhancement in Al-SiO_2-Gr composites can be attributed to a number of factors, including the presence of uniformly distributed harder elements, substantial grain refinement achieved with the addition of SiO_2 + Gr particles, and dislocations generated due to modulus mismatches and differences in thermal expansion coefficients. The results are shown in Fig. 9 which confirms the significant impact of these particles on the fortification of Al-SiO_2-Gr composites by emphasizing the large influence of SiO_2 + Graphene content on the overall compressive strength.

3.5 Hardness Measurements

Figure 10 presents samples of the substrate metal A356 alongside the hybridized composites. Notably, the hybrid composites exhibit higher levels of hardness compared to their unreinforced counterparts, and this hardness demonstrates a consistent upward trend in direct proportion to the weight percentage of the added reinforcement, in alignment with prior investigations [38]. The incorporation of hard reinforcing particles has a dual impact, enhancing both the matrix's hardness and its resistance to plastic deformation [39]. The graph in Figure 10 illustrates the hardness increment up to 7.5%wt. of SiO_2 + Graphene particulates. In particular, the ideal hardness of reinforced composites featuring a mixture surpasses the hardness of unreinforced alloys. This rise in hardness can be attributed to the increased occurrence of hard SiO_2 particles in the aluminum matrix, combined with the inherently high hardness of nano graphene particles [40].

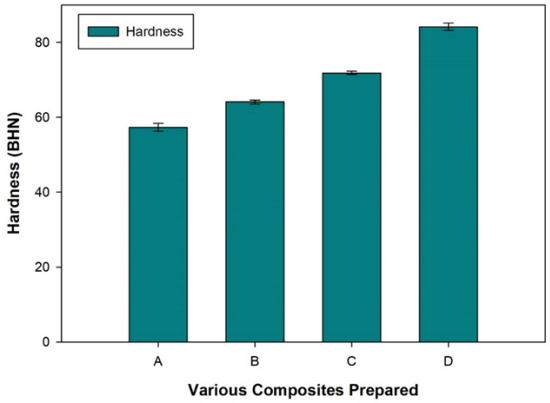

Fig. 10. Hardness of A356 alloy with nano graphene and SiO_2 particles reinforced composites

The introduction of reinforcement particles to the aluminum matrix serves to enhance their surface area, concurrently reducing the size of aluminum matrix grains. This heightened presence of hard surface areas from SiO_2 and nano graphene particles offers substantial resistance to plastic deformation, consequently elevating the overall hardness of the fabricated AMCs. Additionally, the presence of hard and brittle SiO_2 and nano graphene particles within the soft and ductile A356 matrix leads to a reduction in the ductility content of the fabricated AMCs. This reduced ductility within the matrix metal of the composite significantly contributes to the overall hardness of the AMCs. It's worth noting that an increased amount of reinforcement in the matrix results in a higher dislocation density during solidification, attributable to the thermal mismatch between the aluminum matrix and the reinforcement. This discrepancy in thermal expansion creates internal stresses, prompting plastic deformation within the aluminum matrix to accommodate the lower volume expansion of the reinforcement particles. The escalation in dislocation density at the particle-matrix interface intensifies resistance to plastic

deformation, ultimately enhancing hardness. Furthermore, the enhanced hardness observed in hybrid composites can also be ascribed to the observed reduction in porosity, as evident in SEM microphotographs. It is well-documented that higher hardness is closely associated with lower levels of porosity within the MMC. It is evident from the results that the hardness value of the Al-Graphene-SiO_2 hybrid composite surpasses that of other fabricated composites, primarily attributed to the homogeneous distribution of SiO_2 particles within the matrix. The presence of robust SiO_2 particles, in conjunction with the finely dispersed Gr particles, significantly elevates the barriers to grain boundary sliding [41]. Additionally, an essential factor contributing to the overall enhancement in the composite's hardness, owing to the incorporation of SiO_2, stems from an augmented dislocation density due to the thermal expansion mismatch between the reinforcement and the hybrid matrix at the particle-matrix interfaces [42]. The cumulative effect of these factors translates into formidable resistance against localized deformation during indentation.

3.6 Impact Strength

As represented in Fig. 11, the impact strength of the composites exhibits an upward trend in contrast to the unreinforced alloy as the wt. % of SiO_2 + Graphene particles within the metal matrix increases. Nonetheless, it's worth noting that, although the impact strength of hybrid composites shows a tendency to decrease, this reduction is relatively modest. One plausible explanation for the reduction in strength lies in the subtle transformation of material properties from ductile to brittle, which is brought about by the incorporation of hard SiO_2 + Graphene particles. The presence of microstructural defects, resulting from cracking and decohesion of reinforcing particles, contributes to the decline in impact strength within the composites. This decrement in impact strength becomes noticeable with the increasing weight percentage of reinforcement, causing a rise in failure rates. A linear progression in the energy absorbed is evident with the escalation of the reinforcement (SiO_2 + Graphene) weight percentage (Fig. 11). The augmentation in impact energy can be attributed to the reinforcement provided by the robust SiO_2 particles. This rise in impact strength, as indicated by the increasing impact energy, is attributed to the incremental weight percentage of SiO_2 + graphene reinforcements.

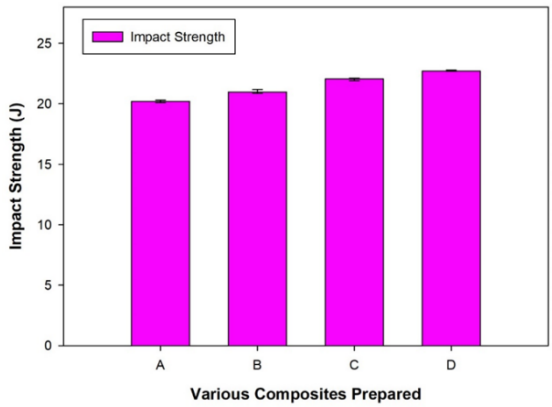

Fig. 11. Impact strength of A356 alloy with nano graphene and SiO_2 particles reinforced composites

4. Conclusion

This paper presents a comprehensive report on the synthesis and microstructural characterization of aluminum matrix composites reinforced with nanographene and SiO_2. The experimental findings have been thoroughly scrutinized, leading to the following key conclusions.

- Successful fabrication of hybrid composites has been attained through the incorporation of SiO_2 and nanographene particles into the aluminum alloy via a liquid metallurgy approach.
- SEM micrographs provide clear evidence of the effective reinforcement of SiO_2 and nanographene, displaying a uniform distribution of particle and robust inter-particle bonding in the base matrix, albeit with minor pore presence.
- Both tensile and yield strength exhibit noticeable increments with the rise in the SiO_2 particles with constant nanographene reinforcement weight percentage in comparison to the as-cast matrix. This surge in strength can be attributed to the reinforcing effect of hard SiO_2 particles and graphene, which contribute to enhanced resistance against tensile loads. The improvements in the ultimate strength of A356 alloy with the 7.5 wt. % of SiO_2 and 1 wt. % of Graphene is 60.64 %. The improvements in the yield strength of A356 alloy with the 7.5 wt. % of SiO_2 and 1 wt. % of Graphene is 82.78 %.
- The percentage elongation decreases as the weight percentage of hybrid reinforcement increases, primarily due to the brittleness introduced by the hard particles and the presence of hard-ceramic particles.
- The compressive strength experiences a notable increase with the augmentation of nanographene and SiO_2 reinforcement weight percentages when compared to the as-cast matrix. Similar to the tensile properties, this increase in strength can be ascribed to the reinforcing impact of hard SiO_2 particles and graphene, which enhance resistance to compressive loads. The improvements in the compressive strength of A356 alloy with the 7.5 wt. % of SiO_2 and 1 wt. % of Graphene is 62.71 %.
- The impact strength of the hybridized composites exhibits a gradual increase with the addition of reinforcement, albeit at a modest rate.
- In the present study 1 wt. % of nano graphene is used along with the varying weight percentages of SiO_2 particles. In the future, the composites with more weight percentages of graphene content can be studied. Also, in the present research mechanical properties were investigated, further various properties can be studied.

References

[1] Suresh S, Shenbaga Vinayaga Moorthi N, Vettivel SC, N. Selvakumar N, Jinu GR. Effect of graphite addition on mechanical behavior of Al6061-TiB2 hybrid composites using acoustic emission, Materials Science and Engineering A, 2014; 612: 16-27. https://doi.org/10.1016/j.msea.2014.06.024

[2] Zeeshan A, Muthuraman V, Rathnakumar P, Guruswamy P, Madeva Nagaral. Influence of B4C particle size on the mechanical behavior of A356 aluminium composites. Research on Engineering Structures and Materials, 2023; 9 (2):527-540.

[3] Ananthakrishna Somayaji, Madeva Nagaral, Chandrashekar Anjinappa, Meshel QA, Ravikiran Kamath Billady, Nithin Kumar, Virupaxi Auradi, Saiful Islam, Ranga Raya CJ, Abdul Razak, Mohammad Amir Khan, Channa Keshava Naik. Influence of graphite particles on the mechanical and wear characterization of Al6082 alloy composites. ACS Omega, 2023; 8(30):26828-26836. https://doi.org/10.1021/acsomega.3c01313

[4] G Kumar, R Saravanan, Madeva Nagaral. Dry sliding wear behavior of nano boron carbide particulates reinforced Al2214 alloy composites. Materials Today: Proceedings, 2023;81:191-195. https://doi.org/10.1016/j.matpr.2021.03.065
[5] Bharath V, Auradi V, Veeresh Kumar GB, Madeva Nagaral, Murthy Chavali, Mahmoud Helal, Rokayya Sami, Aljuraide NI, Jong Wan Hu, Ahmed M Galal. Microstructural Evolution, Tensile Failure, Fatigue Behavior and Wear Properties of Al2O3 Reinforced Al2014 Alloy T6 Heat Treated Metal Composites. Materials, 2022;15(12):4244. https://doi.org/10.3390/ma15124244
[6] Siddesh M., Shivakumar BP, Shashidhar , Nagaral M. Dry sliding wear behavior of mica, fly ash and red mud particles reinforced Al7075 alloy hybrid metal matrix composites. Indian Journal of Science and Technology, 2021;14(4):310-318. https://doi.org/10.17485/IJST/v14i4.2081
[7] Vasanth Kumar HS, Revanna K, Nithin Kumar, Sathyanarayana N, Madeva N, Manjunath GA, Adisu H. Impact of silicon carbide particles weight percentage on the microstructure, mechanical behaviour, and fractography of Al2014 alloy composites. Advances in Materials Science and Engineering, 2022; Article ID 2839150: 1-10. https://doi.org/10.1155/2022/2839150
[8] Krishna UB, Vasudeva B, Virupaxi Auradi, Madeva Nagaral. Effect of Percentage Variation on Wear Behaviour of Tungsten Carbide and Cobalt Reinforced Al7075 Matrix Composites Synthesized by Melt Stirring Method. Journal of Bio-and Tribo-Corrosion, 2021; 7(3):1-8. https://doi.org/10.1007/s40735-021-00528-1
[9] Veeresh Kumar GB, Gude Venkatesh Chowdary, Mandadi Surya Vamsi, Jayarami Reddy K, Madeva Nagaral, Naresh K. Effects of addition of Titanium Diboride and Graphite Particulate Reinforcements on Physical, Mechanical and Tribological properties of Al6061 Alloy based Hybrid Metal Matrix Composites. Advances in Materials and Processing Technologies, 2022;8(2):2259-2276. https://doi.org/10.1080/2374068X.2021.1904370
[10] Ruixiao Zheng, Jing Chen, Yitan Zhang, Kei Ameyama, Chaoli Ma. Fabrication and characterization of hybrid structured Al alloy matrix composites reinforced by high volume fraction of B4C particles, Materials Science and Engineering A, 2014; 601:20-28. https://doi.org/10.1016/j.msea.2014.02.032
[11] Bharath V, Auradi V, Madeva Nagaral, Satish Babu Boppana. Experimental investigations on mechanical and wear behaviour of 2014Al-Al2O3 Composites. Journal of Bio-and Tribo-Corrosion, 2020; 6(2):1-10. https://doi.org/10.1007/s40735-020-00341-2
[12] Massoud Malaki, Alireza Fadaei Tehrani, Behzad Niroumand, Amir Abdullah. Ultrasonically stir cast SiO2/A356 metal matrix nanocomposites. Metals, 2021;11(12):1-18. https://doi.org/10.3390/met11122004
[13] Sekar K, Allesu K, Joseph MA. Effect of heat treatment in tribological properties of A356 aluminium alloy reinforced with Al2O3 nano particles by combination effect of stir and squeeze casting method. Applied Mechanics and Materials, 2014; 592-594: 968-971. https://doi.org/10.4028/www.scientific.net/AMM.592-594.968
[14] Umanath K, Selvamani ST, Palanikumar K, Raphael T, Prashanth K. Effect of sliding distance on dry sliding wear behavior of Al6061-SiC-Al2O3 hybrid composite. Proceedings of International Conference on Advances in Mechanical Engineering, 2013;749-775. https://doi.org/10.1016/j.compositesb.2013.04.051
[15] Dineshkumar SK, Saravanan AK, Raghuram Pradhan, Ramya Suresh, Senthilnathan K. Characterization of Al-SiO2 composite material. International Journal of Engineering and Advanced Technology, 2019; 9(2):2972-2975. https://doi.org/10.35940/ijeat.B3898.129219
[16] Madeva Nagaral, Shaivananda Kalgudi, Auradi V, Kori SA. Mechanical characterization of ceramic nano B4C-Al2618 alloy composites synthesized by semi solid state

processing, Transactions of the Indian Ceramic Society, 2018;77(3):1-4. https://doi.org/10.1080/0371750X.2018.1506363
[17] Dhanalakshmi P, Mohansundararaju N, Venkatkrishnan PG. Preparation and mechanical characterization of stir cast hybrid Al7075 Al2O3 B4C metal matrix composites. Applied Mechanics and Materials, 2014; 592-594: 705-710. https://doi.org/10.4028/www.scientific.net/AMM.592-594.705
[18] Devnani GL, Shishir Sinha. Effect of nano fillers on the properties of natural fiber reinforced polymer composites. Materials Today Proceedings, 2019;18(3):647-654. https://doi.org/10.1016/j.matpr.2019.06.460
[19] Mohammad Narimani, Behnam Lotfi, Zohreh Sadeghian. Evaluation of the microstructure and wear behavior of AA6063-B4C/TiB2 mono and hybrid composite layers produced by friction stir processing. Surface & Coatings Technology, 2016; 285:1-10. https://doi.org/10.1016/j.surfcoat.2015.11.015
[20] Amir Pakdel, Agnieszka Witecka, Gaulthier Rydzek, Dayangku Noorfazidah Awang Shri, Valeria Nicolosi. A comprehensive analysis of extrusion behavior, microstructural evolution and mechanical properties of 6063 Al-B4C composites produced by semisolid stir casting. Materials Science and Engineering Materials A, 2018;721:28-37. https://doi.org/10.1016/j.msea.2018.02.080
[21] Narasimha Murthy I, Venkata Rao D, Babu Rao J. Microstructure and mechanical properties of aluminium fly ash nano composites made by ultrasonic method. Materials and Design, 2012; 35:55-65. https://doi.org/10.1016/j.matdes.2011.10.019
[22] Knowels AJ, Jiang X, Galano M. Microstructure and mechanical properties of 6061 Al alloy based composites with SiC nano particles. Journal of Alloys and Compounds, 2014;615(1):S401-S405. https://doi.org/10.1016/j.jallcom.2014.01.134
[23] Dinesh Kumar Koli, Geeta Agnihotri, Rajesh Purohit. A Review on Properties, Behaviour and Processing Methods for Al-Nano Al2O3 Composites. Procedia Materials Science, 2014; 6:567 - 589. https://doi.org/10.1016/j.mspro.2014.07.072
[24] Mohsen Ostad Shabani. Microstructural and abrasive wear properties of SiC reinforced aluminium based composite produced by compo-casting. Transactions of Nonferrous Metals Society of China, 2013; 23:1905-1914. https://doi.org/10.1016/S1003-6326(13)62676-X
[25] Natarajan N, Vijayarangan S, Rajendran I. Wear behaviour of A356/25 SiCp aluminium matrix composites sliding against automobile friction material. Wear, 2006;261:812-822. https://doi.org/10.1016/j.wear.2006.01.011
[26] Raghu YV, Anil Kumar G, Sateesh J, Madhusudhan T. Investigation of Mechanical properties and Wear rate of Aluminium A356 -SiC MMCs processed by powder metallurgy method. International Research Journal of Engineering and Technology, 2017; 4(8) 444-448.
[27] Mingliang Wang, Dong Chen, Zhe Chen, Yi Wu, Feifei Wang, Naiheng Ma, Haowei Wang. Mechanical properties of in-situ TiB2/A356 composites. Materials Science & Engineering A, 2014; 590:246-254. https://doi.org/10.1016/j.msea.2013.10.021
[28] Shashidhar S, Vijaya Kumar P, Shivananda HK, Madeva Nagaral. Processing, microstructure, density and compression behavior of nano B4C particulates reinforced Al2219 alloy composites. International Journal of Advanced Technology and Engineering Exploration, 2018; 5(46):350-355. https://doi.org/10.19101/IJATEE.2018.546015
[29] Omyma El-Kady, Fathy A. Effect of SiC particle on the physical and mechanical properties o extruded Al matrix composites. Materials and Design, 2014; 54:348-353. https://doi.org/10.1016/j.matdes.2013.08.049
[30] Davis JR. Aluminium and aluminium alloys, ASM specialty handbook, ASM International, 1993.
[31] Vijaya Ramnath B, Elanchezhian C, Jaivignesh M, Rajesh S, Parswajinan C, Siddique Ahmed Ghias A. Evaluation of mechanical properties of aluminium alloy-alumina-

boron carbide metal matrix composites, Materials and Design, 2014; 58:332-338. https://doi.org/10.1016/j.matdes.2014.01.068

[32] Hong SJ, Kim HM, Huh D, Suryanarayana C, Chun BS. Effects of Clustering on the Mechanical Properties of SiC Particulate -Reinforced Aluminum Alloy 2024 Metal Matrix Composites. Material Science and Engineering A, 2003; 347:198-204. https://doi.org/10.1016/S0921-5093(02)00593-2

[33] Al-Qutub AM, Allam IM, Qureshi TW. Wear Properties of 10% Sub-Micron A12O3 / 6061 Aluminum Alloy Composite. International Journal of Applied Mechanics and Engineering, 2002; 7:329-334.

[34] Jayasheel Harti, Prasad TB, Madeva Nagaral, Pankaj Jadhav, Auradi V. Microstructure and dry sliding wear behavior of Al2219-TiC composites, Materials Today Proceedings, 2017;4:11004-11009. https://doi.org/10.1016/j.matpr.2017.08.058

[35] Meijuan Li, Kaka Ma, Lin Jiang, Hanry Hang, Enrique Lavernia, Lianmeng Zhang, Julie Schoenung. Synthesis and mechanical behavior of nanostructured Al5083-TiB2 metal matrix composites. Materials Science and Engineering A, 2016;656:241-248. https://doi.org/10.1016/j.msea.2016.01.031

[36] Balasivanandha Prabu S, Karunamoorthy L, Kathiresan S, Mohan B. Influence of stirring speed and stirring time on distribution of particles in cast metal matrix composite. Journal of Material Processing Technology, 2006; 171:268-273. https://doi.org/10.1016/j.jmatprotec.2005.06.071

[37] Yogesh Prabhavalkar, Chapgaon AN. Effect of volume fraction of Al2O3 on tensile strength of aluminium 6061 by varying stir casting furnace parameters: A review. International Research Journal of Engineering and Technology, 2017; 4(10):1351-1355.

[38] Madeva Nagaral, Shivananda BK, Virupaxi Auradi, Kori SA. Development and mechanical-wear characterization of Al2024-nano B4C composites for aerospace applications. Strength, Fracture and Complexity, 2020; 13(1):1-13. https://doi.org/10.3233/SFC-190248

[39] Bharath V, Ashita DH, Auradi V, Madeva Nagaral. Influence of variable particle size reinforcement on mechanical and wear properties of alumina reinforced 2014Al alloy particulate composite. FME Transactions, 2020;48(4): 968-978. https://doi.org/10.5937/fme2004968B

[40] Raj Kumar, Deshpande RG, Gopinath B, Jayasheel Harti, Madeva Nagaral, Auradi V. Mechanical Fractography and Worn Surface Analysis of Nanographite and ZrO2-Reinforced Al7075 Alloy Aerospace Metal Composites. Journal of Failure Analysis and Prevention, 2021; 21:525-536. https://doi.org/10.1007/s11668-020-01092-5

[41] Madeva Nagaral, Auradi V, Kori SA, Reddappa HN, Jayachandran, Veena Shivaprasad. Studies on 3 and 9 wt. % of B4C particulates reinforced Al7025 alloy composites, AIP conference proceedings, 2017;1859(1):020019. https://doi.org/10.1063/1.4990172

[42] Fazil N, Venkataraman V, Madeva Nagaral. Mechanical characterization and wear behavior of aerospace alloy AA2124 and micro B4C reinforced metal composites. Journal of Metals, Materials and Minerals, 2020;30(4):97-105. https://doi.org/10.55713/jmmm.v30i4.641